この彙報に載せられた論文及び報告についての責任は，すべてその著者のみにある．

この彙報についての照会通信は，すべて東京大学地震研究所長にあてられたい．

The authors of the papers alone are responsible for the statements and opinions contained in their respective papers.

All communications relating to this Bulletin should be addressed to the Director of the Earthquake Research Institute, University of Tokyo, Japan.

Earthquake Research Institute, University of Tokyo
Address:
1-1, Yayoi 1-chome, Bunkyo-ku.
Tokyo, Japan.
Telephone: 812-2111-Extension 5669
Cable address: ZISINKEN, TOKYO

東京大学地震研究所
所在地
東京都文京区弥生1丁目1番1号
電話 812-2111 (大代) 構内 5669
電略 ブンキヨウ トウダイヂシン

BULLETIN OF THE EARTHQUAKE
RESEARCH INSTITUTE
Vol. 57 (1982), pp. 609-625

28. *Spectra of the First Higher Mode of Simulated Oceanic Rayleigh Waves Generated by Deep Earthquakes of the Dip-Slip Type.*

By Mitsuru YOSHIDA,

Earthquake Research Institute.

(Received October 29, 1982)

Abstract

For the purpose of understanding the excitation of the first higher mode of oceanic Rayleigh waves, the waves are simulated for the seismic sources with a pure dip-slip motion along a vertical fault plane, for various focal depths from 10 to 500 km. It is suggested that the first higher mode of oceanic Rayleigh waves generated by deep earthquakes with the focal depth of about 200 or 300 km can be observed in the period range from 20 to 50 seconds, with the amplitude exceeding that of the fundamental mode. The optimum filtering parameters for the analysis of dispersed oceannic Rayleigh waves are determined by using the simulated Rayleigh waves of the fundamental and first higher modes. The filtering parameters will be used most effectively for the determination of the group velocity dispersion curves of oceanic surface waves.

1. Introduction

The velocity of seismic surface waves is, as well as the heat flow, gravity, seismic activity, electrical conductivity and velocity of body waves, one of the essential physical data for the study of the earth's interior. The velocities of the fundamentral modes of Rayleigh and Love waves are often used for the inference of the physical property of rocks constituting the lithosphere and asthenosphere under the ocean or continent, because those fundamental modes are strongly excited by numerous shallow earthquakes, which account for a major portion of seismic events occurring in the earth and are easily observed with long-period seismographs of various types.

On the other hand, the generation, propagation, dispersion and attenuation of higher mode Rayleigh waves were investigated by USAMI, SATÔ

and LANDISMAN (1965) by using theoretical seismograms. It is suggested by HARKRIDER (1970) and FUKAO and ABE (1971) that surface waves of the first higher mode are also useful for the investigation of the underground structure and focal mechanism of earthquakes. The first higher mode of oceanic Rayleigh waves was employed by KOVACH and ANDERSON (1964) for the investigation of the structures near the well-developed low velocity zone under the Pacific.

In the previous paper (YOSHIDA, 1978a) the possibility of the observation of the first higher mode from a 200-km source depth was examined by calculating the medium-response in the period range from 20 to 300 sec in a simple form. If we can compare synthetic seismograms of the first higher mode excited by deep earthquakes with the observation, the analysis of the observed seismograms in the time and frequency domains will effectively progress.

2. Source model and upper mantle structure

At the focus the source is assumed that the focal mechanism is a displacement dislocation with a step-function time dependence and the normal components of stresses are continuous across the fault. The slip dislocation along an infinitesimal fault plane is equivalent to a double couple of body forces without moment (KNOPOFF and GILBERT, 1960; MARUYAMA, 1963; BURRIDGE and KNOPOFF, 1964). The moment of either of the two component couple is called the seismic moment and it is equivalent to the product of the rigidity, the dislocation area of the fault surface and the average dislocation over it (AKI, 1966).

For such a force system radiation patterns of surface waves for vertically heterogeneous elastic media have been derived by several authors (HASKELL, 1964; HARKRIDER, 1964; BEN-MENAHEM and HARKRIDER, 1964; SAITO, 1967; ODAKA and USAMI, 1970) on the basis of the normal mode theory. Using the result of the surface wave excitation theory by SAITO (1967) theoretical seismograms (e. g., KANAMORI, 1970a, b) and theoretical Fourier spectra (TSAI and AKI, 1970) were calculated and compared with the observed waves. In the generation of theoretical seismograms we must take into consideration many factors (USAMI, 1971) such as the focal mechanism, the seismic moment, the structure of medium along the epicenter-station path, the focal depth, the epicentral distance and the attenuation effect of the wave in a dissipated medium.

The factors related to the source and medium mentioned above are selected keeping in mind that, 1) the source mechanism of deep earth-

quakes near the circum-Pacific seismic zone is usually a normal or reverse thrust type, the fault plane dipping close to normal (e. g., HONDA, MASATSUKA and EMURA, 1956; ICHIKAWA, 1960), 2) surface waves travel across the Pacific, and 3) the waves will be observed at the station equiped with the WWSSN long-period seismograph deployed in and around the Pacific.

Seismograms are synthesized by assuming that the source is the pure dip-slip motion along a vertical fault plane with a slip angle 90°. The epicentral distance is 90° in terms of the fault plane geometry and coordinate system in Fig. 1. According to SAITO (1967) and TAKEUCHI and SAITO (1972), the vertical component of displacement for the i th radial harmonics and the n th order ${}_iS_n$ excited by the dip-slip source having the seismic moment of M_0 is given as

$$ {}_iU_n(r, \theta, \phi, t) = M_0 \cdot {}_i\bar{u}_n(r, \theta, \phi) \cdot \cos {}_i\omega_n t \,, \tag{1} $$

where

$$ {}_i\bar{u}_n(r, \theta, \phi) = \sin \phi \cdot \frac{2n+1}{4\pi} \cdot \frac{1}{\mu_s} \cdot y_1(r) \cdot F({}_i\omega_n) \cdot P_n^1(\cos\theta) \cdot y_4(r_s). \tag{2} $$

The transfer function $F({}_i\omega_n)$ is written in the form

$$ F({}_i\omega_n) = 1/[{}_i\omega_n{}^2 \int_0^a \rho r^2 (y_1{}^2 + n(n+1) y_3{}^2) dr] \,. \tag{3} $$

${}_i\omega_n$ is the angular frequency, and r the radial distance from the center of the earth. The source time spectrum of the step-function is multiplied in (3). y_1 and y_3 are the radial factors of the vertical and horizontal components of displacement respectively, y_4 is the radial factors of horizontal component of stress. ρ and μ are the density and rigidity, respectively. The quantity with the subscript s refers to the one at the source. The

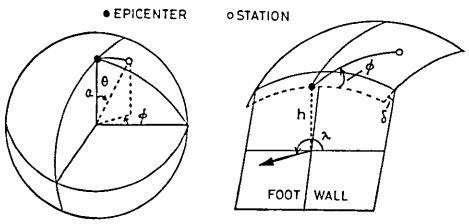

Fig. 1. The coordinate system and fault plane geometry. ϕ is measured from the fault strike direction to the station. The epicenter is assumed to be at the pole $\theta = 0°$. a is the radius of the earth, δ the dip angle, λ the slip angle which specifies the direction of the motion of the hanging wall relative to the foot wall, and h is the focal depth.

first higher mode is calculated in the range of the order number n of the associated Legendre function from 17 to 650, which corresponds to the period range from 280 to 14 sec. To compare its wave forms and spectra the fundamental mode is also generated in the order number of 17 to 900, which corresponds to the period range of 380 to 140 sec.

The oceanic upper mantle model PC-MAX, which was proposed by YOSHIDA (1978b) for the highest-velocity-area in the Pacific on the basis of the group velocity dispersion, was employed as the structure of the medium along the epicenter-station path. Hence the synthesized seismograms will simulate the waves propagating in the western Pacific where the velocity is very high.

The quality factor Q, is rarely reported in the observation for the first higher mode of Rayleigh waves. According to the attenuation data of surface waves (e.g., YAMAKAWA and SATÔ, 1964; NAGAMUNE, SATÔ and SAITO, 1964; BEN-MENAHEM, 1965; ANDERSON, BEN-MENAHEM and ARCHAMBEAU, 1965; SATO, 1967; ABE, SATÔ and FREZ, 1970; KANAMORI, 1970c; SMITH, 1972; NAKANISHI, 1979; YOSHIDA, 1981), the Q values of the fundamental mode of Rayleigh waves vary from 100 to 400 for the period range from 20 to 400 sec.

In the following calculations an intermediate value ${}_0Q_n=200$ is assumed for the fundamental mode, while ${}_1Q_n=400$ for the first higher mode. Higher Q value for the higher mode will be adequate since, compared with the fundamental mode, higher modes are affected by the medium in the deeper part of the earth, where the Q value becomes larger than in the shallower part (ANDERSON and HART, 1978). The expression of the vertical component of displacement including the attenuation effect is written as

$$ {}_iU_n(r, \theta, \phi, t)=M_0 \cdot {}_i\bar{u}_n(r, \theta, \phi) \cdot e^{-i\omega_n t/2 {}_iQ_n} \cdot \cos {}_i\omega_n t \,. \qquad (4) $$

Since the azimuthal angle ϕ measured from the fault strike is assumed to be 90°, Rayleigh waves are most effectively excited.

3. Wave forms of the first higher modes of simulated Rayleigh waves

The synthetic seismograms calculated through the expression (4), in which the seismic moment M_0 of 7.6×10^{27} *dyne-cm* is substituted, are shown in Fig. 2. The value of the seismic moment is the same as that for the Great Kanto earthquake of 1923 (KANAMORI, 1971) and this value is temporarily adopted to see the absolute amplitude of the ground displacement at the epicentral distance 10000 km.

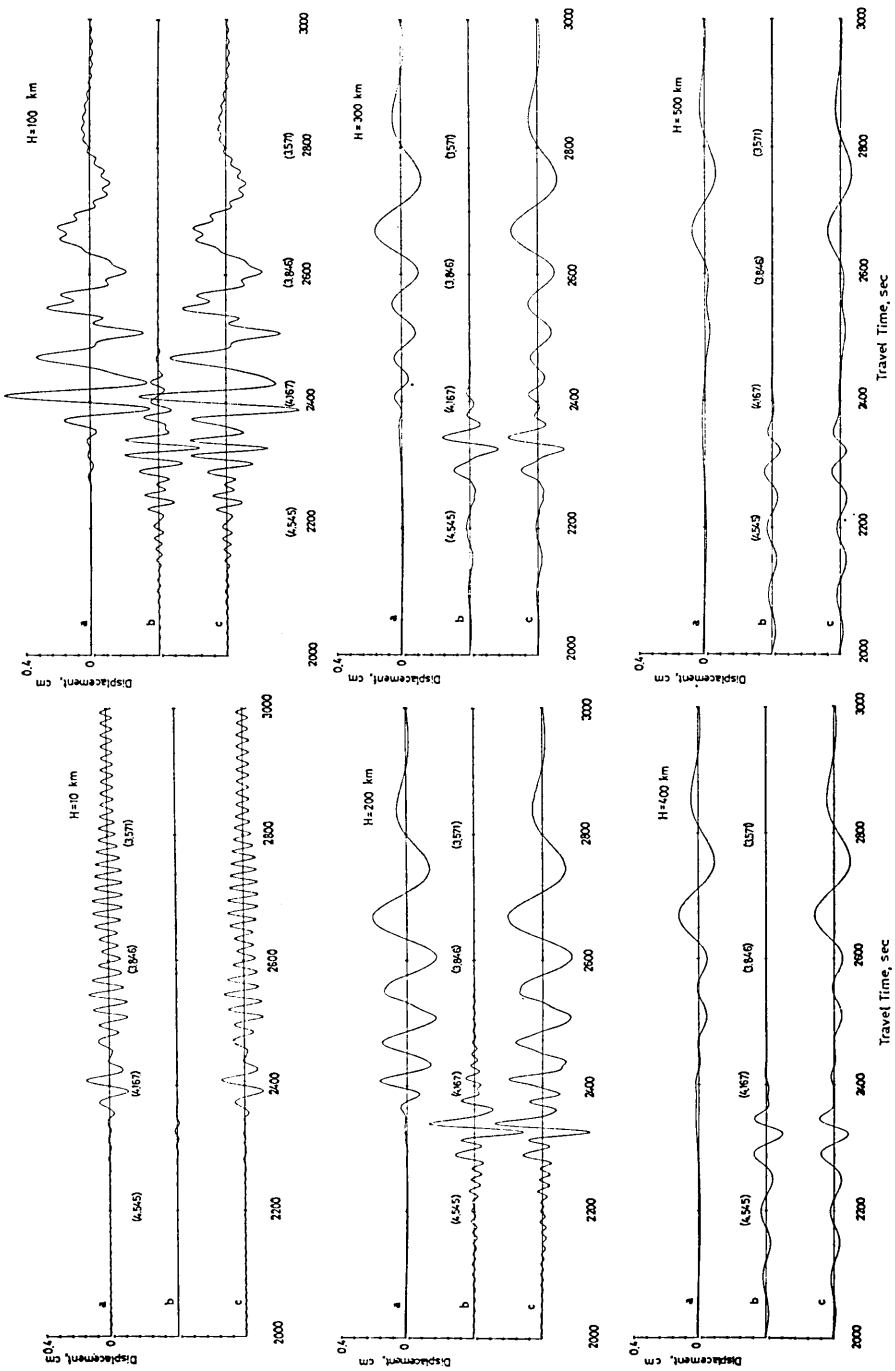

Fig. 2. Theoretical seismograms of oceanic Rayleigh waves of the fundamental mode (a), the first higher mode (b), and the combination of the two modes (c). Both θ and ϕ in the expression (4) are assumed to be ninety degrees. Numerals in the parentheses are the group velocity. H is the focal depth.

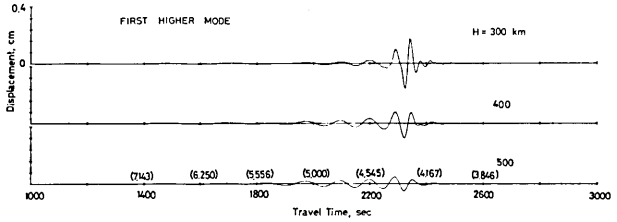

Fig. 3. Theoretical seismograms of oceanic Rayleigh waves of the first higher mode versus the focal depth (H).

We see in Fig. 2 that the excitation of the first higher mode is very weak for a shallow source $H=10$ km and is negligible compared with the fundamental mode, while for the focal depth larger than 100 km the first higher mode is comparable to the fundamental mode. It should be also noted from the same figure that the short-period components of both fundamental and first higher modes decrease with the increase of the focal depth and the two modes overlap each other near the group velocity of 4.20 km/sec. The fundamental mode with the group velocity lower than about 4.20 km/sec is dominated, while the first higher mode with the velocity higher than the value is predominant.

The normal dispersion is clearly seen in the wavetrains of the first higher mode excited by deep sources with the focal depth of 400 and 500 km (Fig. 3) while the fundamental modes from the source depth of 200 and 300 km show a typical anomalous dispersion (Fig. 2). The wavelets composed of the short-period components appear on the first higher mode only for 100 and 200 km source depths and on the fundamental mode only for 10 and 100 km source depths. For the source depth of 400 and 500 km, the first higher and fundamental modes are well seperated on the records.

4. Optimum filtering parameters for the analysis of dispersed oceanic Rayleigh waves

In the analysis of observed surface waves, the calculation of the group or phase velocities in high accuracy is essential. In order to determine the optimum filtering parameters for the analysis of oceanic Rayleigh waves, the group velocity of the fundamental and first higher modes was calculated by the use of the multiple filter technique (DZIEWONSKI, BLOCH and LANDISMAN, 1969). The Gaussian function written below was used as the window function.

$$H_m(\omega)=\begin{cases} 0 & ; \text{ for } \omega<\omega_{l,m} \\ e^{-\alpha((\omega-\omega_m)/\omega_m)^2} & ; \text{ for } \omega_{l,m}\leqq\omega\leqq\omega_{u,m} \\ 0 & ; \text{ for } \omega>\omega_{u,m} \end{cases} \tag{5}$$

and

$$\begin{aligned} \omega_{l,m}&=(1-BAND)\cdot\omega_m \\ \omega_{u,m}&=(1+BAND)\cdot\omega_m\,, \end{aligned} \tag{6}$$

where the parameter $BAND$ is the relative bandwidth, and $\omega_{l,m}$ and $\omega_{u,m}$ are the lower and upper band limits of the symmetrical filter respectively. ω_m is the center freuency. The parameter α in the equation (5) is expressed as

$$\alpha=\beta/BAND^2\,, \tag{7}$$

where β is determined by the function value at the band limits

$$\beta=\ln\left[\frac{H_m(\omega_m)}{H_m(\omega_{l,m})}\right]=\ln\left[\frac{H_m(\omega_m)}{H_m(\omega_{u,m})}\right]. \tag{8}$$

The seismogram generated using the upper mantle PC-MAX was Fourier transformed and the spectrum was multiplied by the Gussian function (5), and we obtained the in-phase spectrum $h_m(\omega)$.

According to GOODMAN (1960), the instantaneous spectral amplitude $A_m(t)$ and phase $\phi_m(t)$ are expressed as

$$A_m(t)\cdot e^{i\phi_m(t)}=h_m(t)+iq_m(t)\,, \tag{9}$$

where $h_m(t)$ and $q_m(t)$ are the in-phase and quadrature time functions. In terms of the Fourier series the quadrature spectrum is related as

$$a_k=-b_k\,,\quad b_k=a_k\,, \tag{10}$$

where a_k and b_k denote the cosine and sine coefficients of the in-phase spectrum.

For synthetic seismograms, the instantaneous spectral amplitudes were calculated at each of the group arrival time for each center frequency ω_m, to determine the dispersion relation of group velocity by employing a set of filtering parameters β and $BAND$. The optimum parameters, which give a satisfactory agreement between the group velocity calculated by the use of the functions (5) and (9) and the theoretical one reported in the previous study (YOSHIDA, 1978b), were determined as $\beta=3.15$ and $BAND=0.15$ ($\alpha=140$) in the period range from 20 to 250 sec.

The group velocity of the first two modes for the focal depth of 200 and 400 km, as determined by employing the filtering parameters men-

tioned above, is shown in Fig. 4. The period range displayed is different between the two modes and between the two focal depths, since as was discussed above the period with the predominant excitation depends not only on the mode but also on the focal depth.

A notable point made clear from Fig. 4 is that at the periods less than 50 sec the first higher mode propagates with a velocity larger than

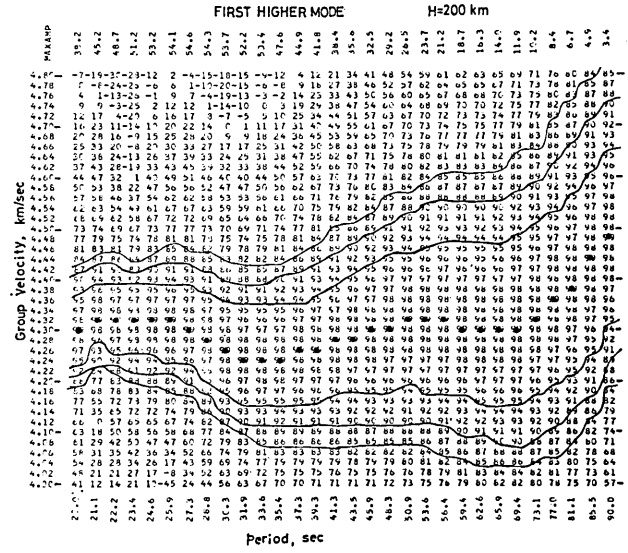

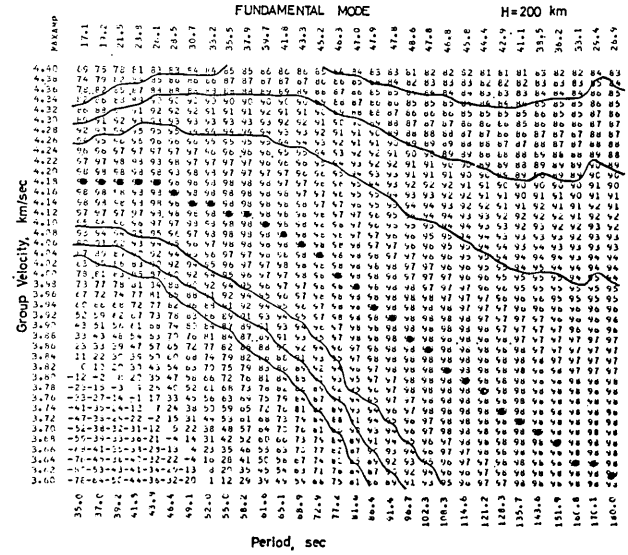

Fig. 4a.

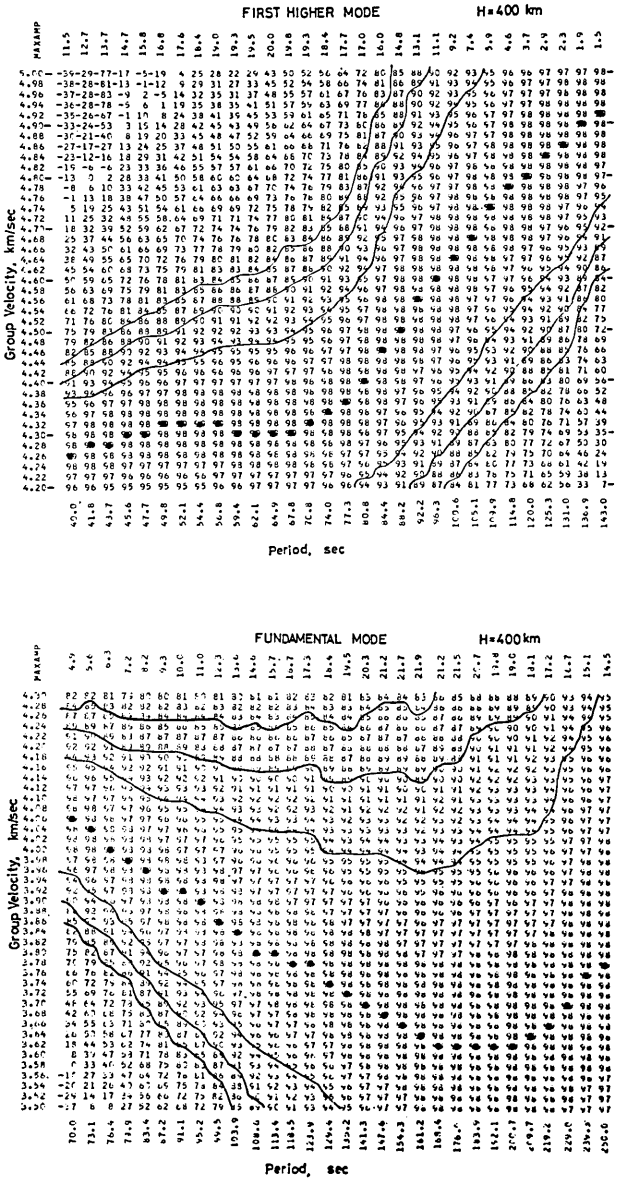

Fig. 4b.

Fig. 4. Group velocities (solid circles) of the first higher and fundamental modes for the focal depths 200 and 400 km. Numerals in the figure are the normalized amplitudes of the instantaneous amplitude spectra in a log scale, the maximum being 99 for each center frequency. The area within the boundary of solid lines shows the velocity range propagating with high energy. The maximum values of the instantaneous amplitude spectra are shown in the top row designated as *MAXAMP* in an arbitrary scale.

4.24 km/sec while the fundamental mode does with a velocity lower than 4.18 km/sec (Fig. 4a). This velocity difference between the two modes makes mode separation easy in a long epicentral distance even if the excitations of them are not so different. Looking at the amplitude of the first higher mode for a 200-km source depth, which is indicated by MAXAMP in the top row in the figure, the excitation in the period range from 20 to 50 sec is very strong.

In the case of the focal depth of 400 km the first higher mode is excited mostly in the period range from 40 to 90 sec, and the group velocity

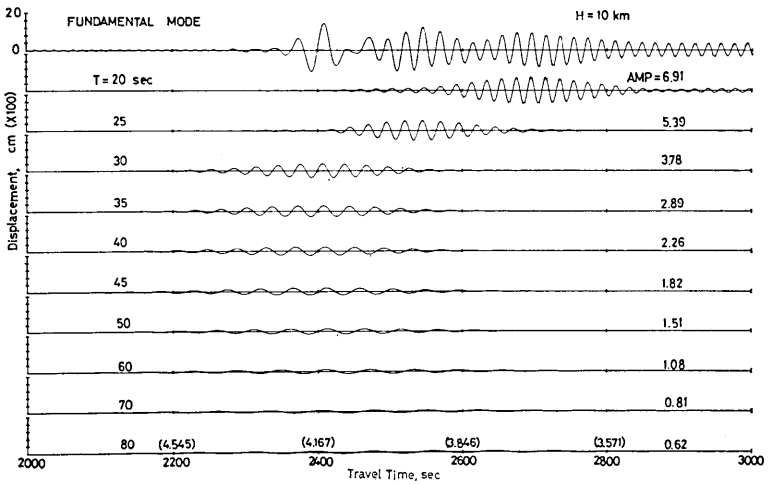

Fig. 5a.

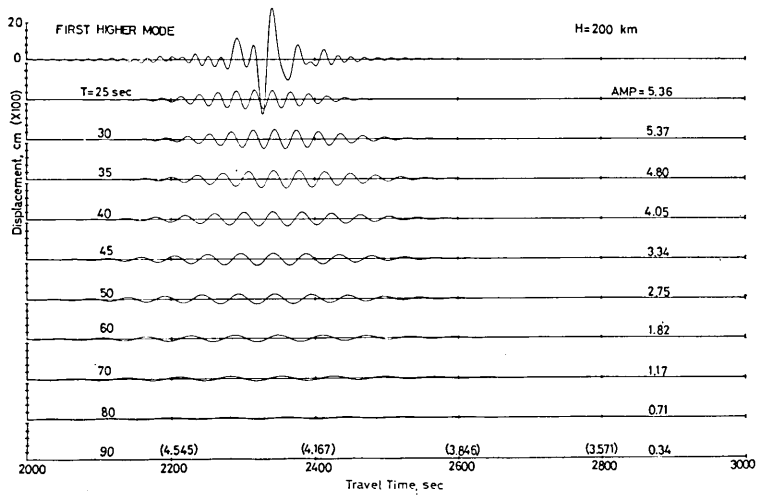

Fig. 5b.

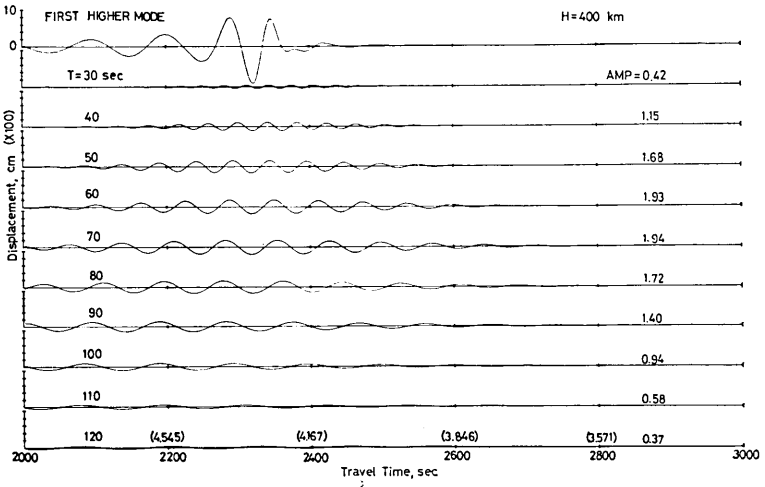

Fig. 5c.

Fig. 5. Band-pass filtered seismograms. T is the wave period and AMP means the maximum half amplitude of each filtered seismogram in an arbitrary scale.

at the period 90 sec is 4.5 km/sec (Fig. 4b), 0.6-km/sec higher than the fundamental mode. Hence compared with the case for a 200-km source depth the mode separation will be easier.

Fig. 5 shows a few examples of the in-phase time function in the expression (9). For a 10-km source depth, the dispersive property of the fundamental mode is well observed from the difference of the arrival times of the band-pass filtered wavetrains. From the traces of the first higher modes for 200- and 400-km source depths we see that the wavetrains show no clear dispersion for periods from 20 to 90 sec.

The energy of the wavetrains, which will be relatively estimated from the amplitude AMP described in the right hand side on the traces, is maximum at 30 sec for a 200-km source depth and at 70 sec for a 400-km source depth, suggesting that the predominant period shifts towards longer periods with increasing focal depth.

5. Spectra of the first higher modes of simulated oceanic Rayleigh waves

The amplitude spectra of the fundamental and first higher modes are shown in Fig. 6. The general spectral patterns of two modes can be explained by the scaling law of surface wave spectra between the spectral peak period (T_p) and the focal depth (H), which is related as

$$T_p = \frac{\lambda}{C} \sim \frac{H}{U}, \tag{11}$$

where λ is the wave length, and C and U are the phase and group velocities respectively.

Namely, the spectral peak of the first higher mode is shorter than that of the fundamental mode since the velocity of the former is faster than that of the latter, and in the two modes the spectral peaks shift towards longer periods with increasing focal depth.

It should be noted that, in the first higher mode, the intensity of the amplitude spectra for a 10-km source depth is remarkably small, less than 10% of that for a 100-km depth in the period range from 20 to 300 sec (Fig. 6b). In the fundamental mode it is an interesting phenomenon that the spectra for a 10-km source depth are forming a cusp, with the spec-

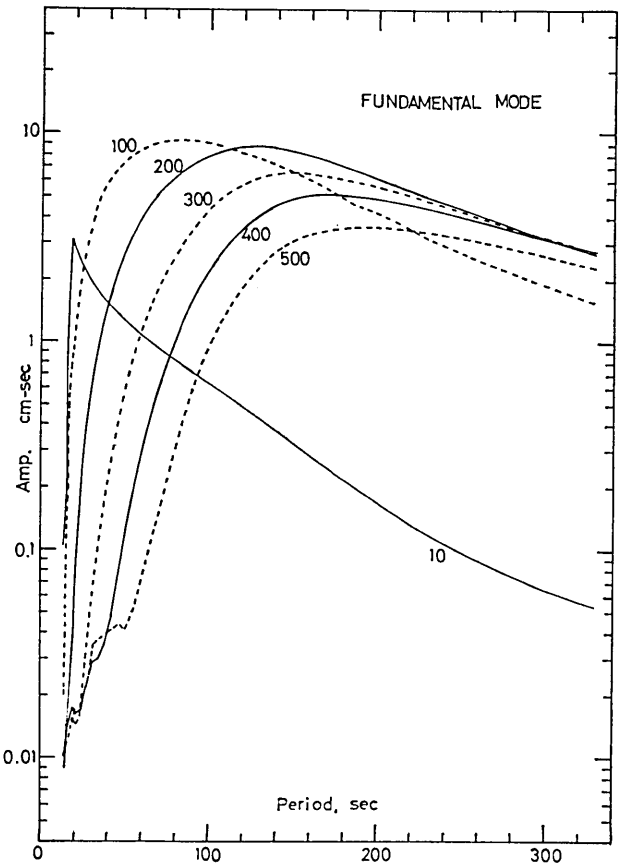

Fig. 6a

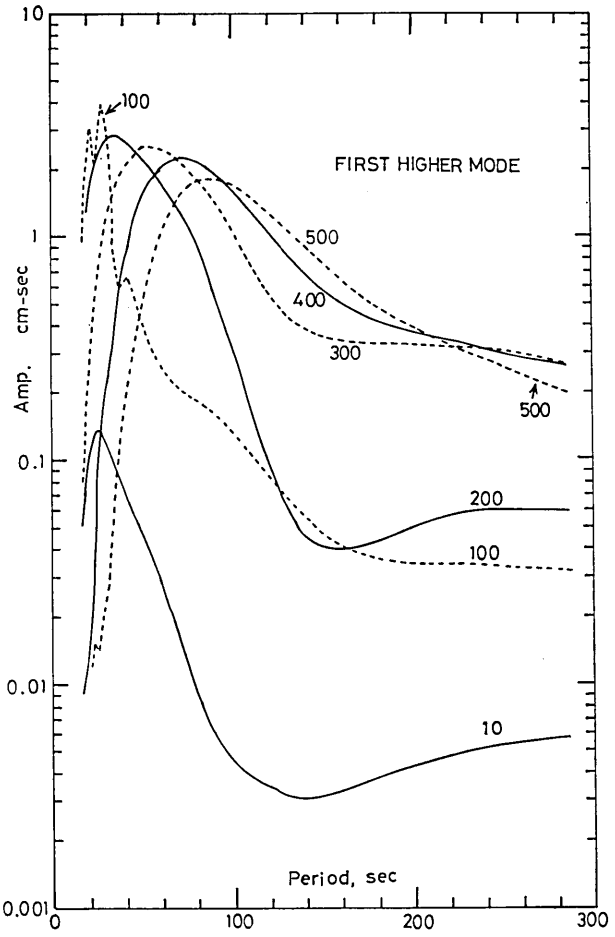

Fig. 6b.

Fig. 6. Amplitude spectra of the fundamental and first higher modes shown in Fig. 2. The ordinate is given in an arbitrary scale.

tral peak located near the period 10 sec. This peculiar spectra may be caused by the situation that the focal depth is located near the boundary layer between oceanic crust and upper mantle (Fig. 6a).

Fig. 7 shows that there is a period range in which the excitation of the first higher mode is stronger than the fundamental mode for the focal depth larger than 100 km. The period ranges approximately from 20 to 30, 50, 70, 90, and 30 to 110 sec for the focal depth of 100, 200, 300, 400, and 500 km respectively. ARKHANGEL'SKAYA (1977) found some relations similar to those mentioned above, by analyzing observed Rayleigh waves of the fundamental and first higher modes propagating in a continent, and used

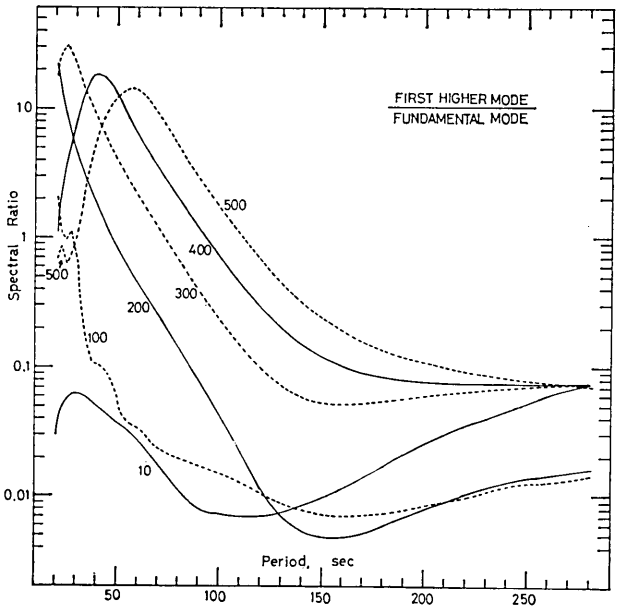

Fig. 7. Amplitude spectral ratio of the first higher mode to the fundamental mode. Numerals attached to the solid or dotted lines indicate the focal depth in km.

the spectral ratios of two modes mainly for the purpose of the determination of the focal depth.

From the theoretical analyses of the amplitude spectra and velocity analyses we can say that i) for deep earthquakes the excitation of the first higher mode is comparable or superior to that of the fundamental mode in a part of the period range from 20 to 110 sec, and ii) the wavetrains of the first higher mode separate from those of the fundamental mode with increasing focal depth and increasing wave period of Rayleigh waves.

So far we made synthetic seismograms assuming constant Q values of 200 and 400 for the fundamental and first higher modes, respectively. If we use the frequency-dependent Q value in the expression (4) the amplitude of the two modes will become somewhat different. In facts, the observed Q value for the fundamental mode is slightly lower in the period range from 20 to 300 sec and higher at the periods longer than 300 sec (SMITH, 1972) and the similar trend will be expected for the first higher mode. Hence, even if we take the frequency-dependent Q value into consideration for the generation of synthetic seismograms, the pattern of the spectral ratio of the first higher mode to the fundamental mode will be

characterized as shown in Fig. 7 approximately.

The results obtained above with respect to the features of the first higher mode through synthetic seismograms will be useful for the studies of the upper mantle structures under the ocean, the focal mechanism of deep earthquakes and the propagation of multi-mode Rayleigh waves.

Acknowledgments

The author wishes to thank Profs. T. Usami, T. Maruyama and Dr. R. Yamaguchi for their valuable discussions and suggestions in the early stage of this work. He is grateful to Prof. M. Saito for his valuable comments.

References

ABE, K., Y. SATÔ and J. FREZ, 1970, Free oscillations of the earth excited by the Kurile Island earthquake 1963, *Bull. Earthq. Res. Inst.*, **48**, 87-114.

AKI, K., 1966, Generation and propagation of *G* waves from the Niigata earthquake of June 16, 1964, Part 2. Estimation of earthquake moment, released energy, and stress-strain drop from the *G* wave spectrum, *Bull. Earthq. Res. Inst.*, **44**, 73-88.

ANDERSON, D. L., A. BEN-MENAHEM and C. B. ARCHAMBEAU, 1965, Attenuation of seismic energy in the upper mantle, *J. Geophys. Res.*, **70**, 1441-1448.

ANDERSON, D. L. and R. S. HART, 1978, *Q* of the earth, *J. Geophys. Res.*, **83**, 5869-5882.

ARKHANGEL'SKAYA, V. M., 1977, The fields of the principal mode and harmonics of Rayleigh surface waves from earthquake of various focal depths, *Physics of the Solid Earth*, **13**, 218-222.

BEN-MENAHEM, A. and D. G. HARKRIDER, 1964, Radiation patterns of seismic waves from buried dipolar point sources in a flat stratified earth, *J. Geophys. Res.*, **69**, 2605-2620.

BEN-MENAHEM, A., 1965, Observed attenuation and *Q* values of seismic surface waves in the upper mantle, *J. Geophys. Res.*, **70**, 4641-4651.

BURRIDGE, R. and L. KNOPOFF, 1964, Body force equivalents for seismic dislocations, *Bull. Seism. Soc. Amer.*, **54**, 1875-1888.

DZIEWONSKI, A., S. BLOCH and M. LANDISMAN, 1969, A technique for the analysis of transient seismic signals, *Bull. Seism. Soc. Amer.*, **59**, 427-444.

FUKAO, Y. and K. ABE, 1971, Multi-mode Love waves excited by shallow and deep earthquakes, *Bull. Earthq. Res. Inst.*, **49**, 1-12.

GOODMAN, N. R., 1960, Measuring amplitude and phase, *J. Franklin Inst.*, **270**, 437-450.

HARKRIDER, D. G., 1964, Surface waves in multilayered elastic media, 1, Rayleigh and Love waves from buried sources in a multilayered elastic half-space, *Bull. Seism. Soc. Amer.*, **54**, 627-679.

HARKRIDER, D. G., 1970, Surface waves in multilayered elastic media. Part II. Higher mode spectra and spectral ratios from point sources in plane layered earth models, *Bull. Seism. Soc. Amer.*, **60**, 1937-1987.

HASKELL, N. A., 1964, Radiation pattern of surface waves from point sources in a multilayered medium, *Bull. Seism. Soc. Amer.*, **54**, 377-393.

HONDA, H., A. MASATSUKA and K. EMURA, 1956, On the mechanism of the earthquakes and stresses producing them in Japan and its vicinity (Second Paper), *Science Reports, Tohoku Univ. Ser 5, Geophys.*, 8, 186-205.

ICHIKAWA, M., 1960, On the mechanism of the earthquakes in and near Japan during the period from 1950 to 1957, *Geophys. Mag.*, **30**, 355-403.

KANAMORI, H., 1970a, The Alaska earthquake of 1964: Radiation of long-period surface waves and source mechanism, *J. Geophys. Res.*, **75**, 5029-5040.

KANAMORI, H., 1970b, Synthesis of long-period surface waves and its application to earthquake source studies-Kurile Island earthquake of October 13, 1963, *J. Geophys. Res.*, **75**, 5011-5027.

KANAMORI, H., 1970c, Velocity and Q of mantle waves, *Phys. Earth Planet. Interiors*, **2**, 259-275.

KANAMORI, H., 1971, Faulting of the Great Kanto Earthquake of 1923 as revealed by seismological data, *Bull. Earthq. Res. Inst.*, **49**, 13-18.

KNOPOFF, L. and F. GILBERT, 1960, First motions from seismic sources, *Bull. Seism. Soc. Amer.*, **50**, 117-134.

KOVACH, R. L. and D. L. ANDERSON, 1964, Higher mode surface waves and their bearing on the structure of the earth's mantle, *Bull. Seism. Soc. Amer.*, **54**, 161-182.

MARUYAMA, T., 1963, On the force equivalents of dynamical elastic dislocations with reference to the earthquake mechanism, *Bull. Earthq. Res. Inst.*, **41**, 467-486.

NAGAMUNE, T., Y. SATÔ and M. SAITO, 1964, Short period free oscillation of the earth caused by the Chilean earthquake of May 22, 1960 and related problems., *J. Phys, Earth*, **12**, 37-41.

NAKANISHI, I., 1979, Phase velocity and Q of mantle Rayleigh waves, *Geophys. J. R. Astr. Soc.*, **58**, 35-59.

ODAKA, T. and T. USAMI, 1970, Theoretical seismograms and earthquake mechanism Part III. Azimuthal variation of the initial phase of surface waves, *Bull. Earthq. Res. Inst.*, **48**, 669-689.

SAITO, M., 1967, Excitation of free oscillations and surface waves by a point source in a vertically heterogeneous earth, *J. Geophys. Res.*, **72**, 3689-3699.

SATO, R., 1967, Attenuation of seismic waves, *J. Phys. Earth*, **15**, 32-61.

SMITH, S. W., 1972, The anelasticity of the mantle, *Tectonophysics*, **13**, 601-622.

TAKEUCHI, H. and M. SAITO, 1972, Seismic surface waves, in *Method in Computational Physics*, edited by B. A. Bolt, 217-295, Academic Press.

TSAI, Y. B. and K. AKI, 1970, Precise focal depth determination from amplitude spectra of surface waves, *J. Geophys. Res.*, **75**, 5729-5743.

USAMI, T., Y. SATÔ and M. LANDISMAN, 1965, Theoretical seismograms of spheroidal type on the surface of a heterogeneous sherical earth, *Bull. Earthq. Res. Inst.*, **43**, 641-660.

USAMI, T., 1971, Theoretical seismograms and earthquake mechanism Part IV. Effect of focal depth, dip angle and fault type on surface waves and surface wave magnitude, *J. Phys. Earth*, **19**, 289-302.

YAMAKAWA, N. and Y. SATÔ, 1964, Q of surface waves, *J. Phys. Earth*, **12**, 5-18.

YOSHIDA, M., 1978a, Velocity and response of higher mode Rayleigh waves for the Pacific Ocean, *Bull. Earthq. Res. Inst.*, **53**, 1135-1150.

YOSHIDA, M., 1978b, Group velocity distributions of Rayleigh waves and two upper mantle models in the Pacific Ocean, *Bull. Earthq. Res. Inst.*, **53**, 319-338.

YOSHIDA, M., 1981, Attenuation characteristics and phase velocity of long-period Rayleigh waves, *Bull. Earthq. Res. Inst.*, **56**, 641-652.

28. 縦ずれ型深発地震によって励起される合成海洋性レイリー波の一次高次モードのスペクトル

地震研究所　吉田　満

海洋性一次高次モードレリー波の励起について理解する為に，震源の深さを 10 km から 500 km まで数多くとり，純粋な縦ずれ断層型の震源を仮定して合成波を得た．それによれば，震源の深さが約 200 km から 300 km の深発地震によって生成される海洋性一次高次モードレイリー波は周期20秒から50秒の範囲で観測可能である事が期待され，その振幅は基本モードを越えている．分散した海洋性レイリー波を解析する為の最適フィルタリングパラメータが，合成された基本及び一次高次モードレイリー波を使って決定された．このフィルタリングパラメータは海洋性表面波の群速度分散曲線決定の際に最も効果的に使われる．